Trapping Ultracold Dysprosium: A Highly Magnetic Gas for Dipolar Physics

Mingwu Lu, Seo Ho Youn, and Benjamin L. Lev

Department of Physics, University of Illinois at Urbana-Champaign, Urbana, Illinois 61801-3080, USA

Ultracold dysprosium gases, with a magnetic moment 10 times that of alkali atoms and equal only to terbium as the most magnetic atom, are expected to exhibit a multitude of fascinating collisional dynamics and quantum dipolar phases, including quantum liquid crystal physics. We report the first laser cooling and trapping of half a billion Dy atoms using a repumper-free magneto-optical trap (MOT) and continuously loaded magnetic confinement, and we characterize the trap recycling dynamics for bosonic and fermionic isotopes. The first inelastic collision measurements in the few partial wave, 100 μK–1 mK, regime are made in a system possessing a submerged open electronic f shell. In addition, we observe unusual stripes of intra-MOT <10 μK sub-Doppler cooled atoms.

Ultracold gases of extraordinarily magnetic atoms, such as dysprosium, offer opportunities to explore strongly correlated matter in the presence of the long-range, anisotropic dipole-dipole interaction (DDI). Such interactions can compete with short-range interactions to induce phases beyond those described by the nearest neighbor Hubbard model [1]. Specifically, quantum liquid crystal (QLC) physics [2] describes strongly correlated systems in which a Fermi surface can spontaneously distort (nematics) or cleave into stripes (smectics) [3]. While material complexity can inhibit full exploration of QLC phases in condensed matter, QLC phases may be more extensively characterized in tunable ultracold gases. In contrast to ultracold ground state polar molecules [4], ultracold Dy offers the ability to explore the spontaneously broken symmetries inherent in QLCs since the DDI is realized without a polarizing field. An exciting prospect lies in observing spontaneous magnetization, e.g., a quantum ferronematic phase in ultracold fermionic Dy gases not subjected to a polarizing field [5].

We report the first magneto-optical trap (MOT) and ultracold collisional rates of this highly complex atom. The stable atoms possessing the largest magnetic moments are the neighboring lanthanide rare earths, Tb and Dy [both 10 Bohr magnetons (μ_B) to within 0.6% [6,7]]. Prior to this work, the coldest Dy was achieved via buffer gas and adiabatic cooling to 50 mK with final densities of $<10^9$ cm^{-3} [8], and Dy beams have been cooled in a single transverse direction via photon scattering [9,10].

Experiments using degenerate ^{52}Cr, a bosonic S-state atom with $\mu = 6\mu_B$, have begun to explore quantum ferrofluids [11]. Experimental access beyond the superfluid and Mott insulator regions of the extended Bose-Hubbard phase diagram to the density wave and supersolid regimes [12] requires a large DDI-to-contact interaction ratio ($\propto\mu^2 m/a_s$, with mass m and scattering length a_s) likely unreachable in the Cr system [11,12]. In contrast, the 9$\times$ larger $\mu^2 m$ in Dy will allow access to these exotic lattice phases provided a suitable a_s exists.

New research avenues include exploration of dipolar Bose-Fermi mixtures of near equal mass, studies of degenerate spinor gases [13] with large spins, and simulations of dense nuclear matter [14]. Ultracold Dy will aid precision measurements of parity nonconservation and fundamental constant variation [9], single-ion implantation [15], and quantum information science [16]. The telecommunications band (1322 nm) and InAs quantum dot-amenable (1001 nm) transitions (Fig. 1) will enable atom-photonic or atom-quantum dot hybrid quantum circuits. Novel collisional [17] and molecular physics are expected among these dipolar $L \neq 0$ atoms possessing submerged open f shells inside closed 5s and 6s electron shells.
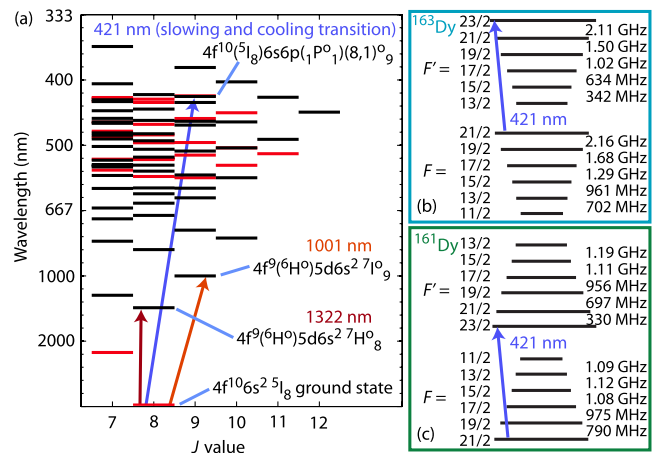

FIG. 1 (color online).　(a) Dy energy level structure [6,25]. MOT and Zeeman slower employ the strongest laser cooling transition (421 nm) between the even parity (red) ground state and the odd (black) excited state. Dy's five high-abundance isotopes: bosons ^{164}Dy, ^{162}Dy, and ^{160}Dy with $I = 0$; and fermions ^{163}Dy and ^{161}Dy with $I = 5/2$. (b),(c) Fermion hyperfine structure (not to scale); $F = J + I$.

The repumperless Dy MOT forms in a similar fashion to the Er ($7\mu_B$) MOT [15]: strongly dipolar Dy remains magnetically trapped in the MOT region while excited state population decays through metastable states. No repumping lasers are necessary because atoms recycle to the MOT from the magnetic quadrupole trap (MT).

The Dy cooling and trapping apparatus consists of a high temperature oven, transverse cooling stage, Zeeman slower, and MOT region. We elaborate on the design elsewhere [18]. Dy nuggets in an apertured 1250 °C Ta crucible provide the atomic beam. Three ion pumps—located at the oven, transverse pumping stage, and MOT chamber—along with titanium sublimation, achieve a vacuum of 1.8×10^{-11} Torr during MOT operation. The atomic beam passes through a differential pumping tube before intersecting four 100 mW, 2 cm-long transverse cooling beams detuned -0.2Γ from the 421-nm transition [19]. Transverse cooling enhances the optimized MOT population by a factor of 3–4. The atomic beam then passes through a spin-flip Zeeman slower [10] operating at -24Γ. The power of the Zeeman slowing laser is >1 W at the slower entrance; we find a linear increase in MOT population until ~ 1 W. Atoms in the slowed beam are captured by a 6-beam MOT with detuning $\delta = -\Gamma$, 1.1-cm beam waists, and total intensity $I = 36$ mW/cm². A 35 G/cm magnetic quadrupole gradient $\nabla_z B \approx 2\nabla_x B$ realizes maximum MOT population. The 421-nm lasers are derived from two doubled Ti:sapphire lasers transfer cavity locked to a Rb-stabilized diode laser.

Steady state bosonic Dy MOT populations form in proportion to natural abundance. However, the MOT population of fermions ^{163}Dy and ^{161}Dy are $5/6\times$ and $1/6\times$ the expected, respectively, which is likely due to poor optical pumping to the $F = 21/2$ ground state [18].

Figure 2(a) describes our model of the Dy MOT recycling mechanism, which is a refinement of that proposed for the Er MOT [15]. The blue cooling laser excites a fraction $f_{ex} < 1/2$ of the population to the 421-nm level, where it can decay with branching ratio R_1/Γ to the metastable states. Upon decay, a fraction pf_{ex} of the population is captured in the MT of the MOT at rate $pf_{ex}R_1$. MOT recycling data, examples of which are shown in Figs. 2(b) and 2(c), support a dual decay path through the dark metastable states; with probability q $(1 - q)$ the population decays through the slow (fast) branch at rate R_{slow} (R_{fast}). Population that reaches the ground state reloads the MOT at rate R_{reload}, which depends on MOT parameters.

There are two loss rates from the otherwise closed system (once loading from the Zeeman slower ceases). A portion of the MOT population can decay to nonmagnetically trapped metastable states at rate $R_{loss\,MOT} = (1 - p)f_{ex}R_1$. Additionally, metastable and ground state MT populations can be lost due to background and two-body inelastic collisions. Two-body loss is difficult to
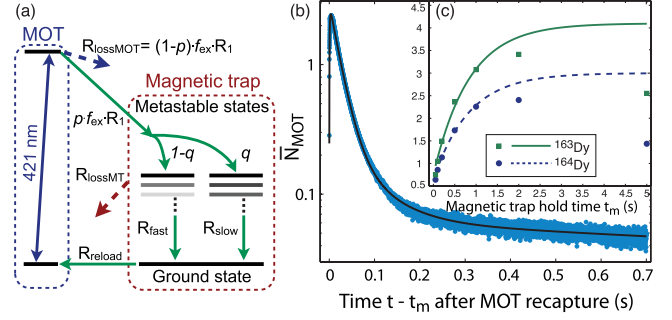

FIG. 2 (color online).   (a) Dy MOT recycling and continuously loaded MT schematic. (b) Population ratio $\bar{N}_{MOT}$ of recaptured MOT to steady state MOT. Black line is fit using Eqs. (1) to $\bar{N}_{MOT}$ with Zeeman slower and atomic beam off, and $t_m = 1$ s delay between steady state MOT and recapture. Inset (c) plots the peak recaptured MOT population versus hold time in MT. Lines are fits to $t \leq 1$ s data with exponential time constants $[R_{slow}^{163}, R_{slow}^{164}] = [1.5, 2.3]$ s^{-1} and extended to later times for comparison. $\bar{N}_{MOT} < 1$ at early times is due to the initial $N_{fast} \neq 0$.

quantify in the metastable states, but we investigate ground state MT loss below: R_{slow} is faster than the ground state component of $R_{loss\,MT}$, and we neglect $R_{loss\,MT}$ in the following rate equations.

Adapting the procedure outlined in Ref. [15], the rates in the MOT recycling model are determined by fitting rate equations to sets of MOT decay transients, e.g., Fig. 3(b), taken at various combinations of MOT beam intensity and detuning:

$$
\begin{aligned}
\dot{N}_{MOT} &= R_{reload}N_{MT} - f_{ex}R_1 N_{MOT}, \\
\dot{N}_{fast} &= (1 - q)pf_{ex}R_1 N_{MOT} - R_{fast}N_{fast}, \\
\dot{N}_{slow} &= qpf_{ex}R_1 N_{MOT} - R_{slow}N_{slow}, \\
\dot{N}_{MT} &= R_{fast}N_{fast} + R_{slow}N_{slow} - R_{reload}N_{MT},
\end{aligned}
\tag{1}
$$

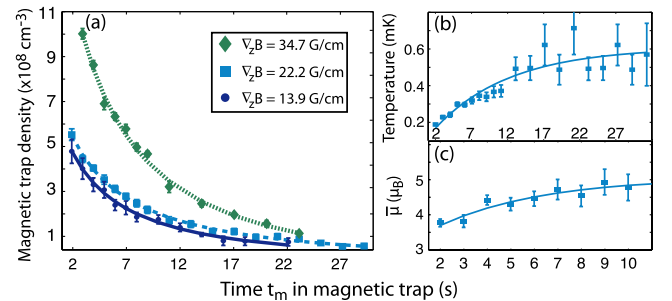where N_{MOT}, N_{fast}, N_{slow}, and N_{MT} are the populations of

FIG. 3 (color online).   (a) Decay of magnetic trap mean density for three gradients. Density profiles are consistent with a single thermal distribution after $t_m = 2$ s. Data are fit to obtain one (γ) and two-body (β) collisional loss rates. (b) Heating in $\nabla_z B = 22.2$ G/cm magnetic trap. (c) Increase in mean magnetic moment $\bar{\mu}$ for the same trap. An exponential fit gives a $\bar{\mu}(t)$ time constant of $\tau = 0.22(5)$ s^{-1}.

the MOT, fast (slow) metastable state decay channel, and MT, respectively. To define initial conditions, the MOT is loaded with the Zeeman slowed atomic beam until reaching steady state, then the MOT, slower, and atomic beams are extinguished for $t_m = 1$ s, during which most of the population in the metastable states decay to the ground state. The population equations are numerically fit to the data for 9 (8) combinations of MOT power and detuning for the fermion ^{163}Dy (boson ^{164}Dy). The hold time t_m in the MT is sufficiently long that residual population in N_{slow} does not affect fit results; all other variables are free to vary. R_1 is extracted from the product $R = f_{ex}R_1$ by simultaneously fitting the R's for each isotope to the function $R(I, \delta) = R_1\bar{I}/(2 + 2\bar{I} + 2(2\delta/\Gamma)^2)$, where $\bar{I} = I/I_s$ and $I_s \approx 2.7 \times 58$ mW/cm^2 in the MOT.

Averaging the results, we find that for both isotopes

$$[R_1^{163}, R_{fast}^{163}, R_{slow}^{163}] = [1170(20), 19(2), 1.5(1)] \text{ s}^{-1},$$

$$[R_1^{164}, R_{fast}^{164}, R_{slow}^{164}] = [1700(100), 29(1), 2.3(1)] \text{ s}^{-1},$$

and $[p, q] = [0.82(1), 0.73(1)]$. The R_1^{164} rate is consistent with the corresponding bosonic ^{168}Er ($I = 0$) MOT quantity, and we suggest that the isotope-induced difference in Dy MOT decay rates arises from ^{163}Dy's hyperfine structure. Dy Zeeman slowing and MOT collection is possible because of the small branching ratio 7×10^{-6} [20]. The p and q values indicate that 82% of the atoms are captured by the MT and 73% of those cascade through the slow channel. Dy level linewidths are mostly unknown, but we speculate that much of this population is captured by the long-lived states near the 1322-nm telecom transition.

Using the measured R_{slow} rates as fixed constants, data of the maximum MOT recapture population [peaks of data in, e.g., Fig. 2(b)] versus t_m are fit to an exponential with only the initial and final MOT population as free variables. Good fits are obtained for $t_m \lesssim 1$ s data, and Fig. 2(c) shows that population in the steady state MOT is only a fraction of the total number of trapped atoms. The "hidden" population in the continuously loaded MT is several times larger, filling the ground state MT at rate R_{slow}. Compared to the steady state MOT, nearly 2.5× (3.5×) more ^{164}Dy (^{163}Dy) atoms are in the recaptured MOT. At optimal MOT parameters and after $t_m = 2$ s of MT loading, we measure the total population of laser cooled and trapped atoms to be 5×10^8 for ^{164}Dy and 3×10^8 for ^{163}Dy. Populations are measured via fluorescence collection on a fast photodiode with atom number calibration to $\leq 10\%$ from absorption imaging [18].

Population loss at times $t_m > 1$ s is likely due to background and inelastic collisions of ground state atoms in the MT. (Majorana spin-flip losses are negligible at these t_m's and trap densities.) We investigate these collision rates by absorption imaging the atoms confined in the MT at various t_m delay times. After loading the MOT, we extinguish the MOT, Zeeman slower, and atomic beams while maintaining a constant ∇B. The MT is turned off at t_m, and after

1 ms, an absorption image integrates on a 16-bit CCD camera for 200 μs. Accounting for gravity $-g\hat{z}$, the images taken in the x-z plane containing the quadrupole axis (along $\hat{z}$) are fit to

$$p_x(x) \propto \exp(-2|x|\sqrt{1 - \bar{g}^2}/\bar{x})(1 + 2|x|\sqrt{1 - \bar{g}^2}/\bar{x}),$$

$$p_z(z) \propto \exp(-2|z|/\bar{z} - 2\bar{g}z/\bar{z})(1 + 2|z|/\bar{z}),$$

where $\bar{g} = mg/(\bar{\mu}\nabla_z B)$, $\bar{\mu}$ is the mean μ of the atomic cloud, and $[\bar{x}, \bar{z}] = 2k_B T/(\bar{\mu}\nabla_{x,z}B)$ [21]. We extract the mean cloud density n, temperature T, and $\bar{\mu}$ versus t_m, which are plotted in Fig. 3 for several MT gradients.

The ^{164}Dy density decay data in Fig. 3(a) are fit to the one plus two-body decay equation $\dot{n} = -\gamma n - \beta n^2$, where γ is the loss rate due to background collisions and β is a measure of inelastic two-body losses. For the three trap gradients, the extracted β's and γ's are consistent with one another within 1σ; the weighted means are $[\bar{\beta}, \bar{\gamma}] = [2.1(2) \times 10^{-10} \text{ cm}^3/\text{s}, 5.6(3) \times 10^{-2} \text{ s}^{-1}]$. Fitting the data to $\dot{n} = -\beta n^2$ results in a worse χ^2. Temperature heating data—e.g., Fig. 3(b)—are fit to an exponential, resulting at early times to a heating rate of 17(2) μK/s, which is consistent with heating rates in spin unpolarized Er and Cr MTs [21,22] and is likely due to spin-relaxation collisions. The MT population is initially distributed among weak-field seeking Zeeman states, and spin exchange collisions tend to polarize the sample toward $m_J = 8$. Indeed, $\bar{\mu}$ increases with time [Fig. 3(c)], and $\bar{\mu}(t)$ reaches 8 μ_B within $t_m = 4$ s in the high gradient $\nabla_z B = 34.7$ G/cm trap.

The measured $\bar{\beta}$ is likely due to an unresolved combination of inelastic spin exchange, magnetic dipole-dipole relaxation (MDDR), and anisotropic electrostatic-driven spin-relaxation collisions. Compared to $\beta_{Cr} = 3 \times 10^{-11}$ cm^3/s in 200 μK spin-polarized ^{52}Cr [22], $\bar{\beta}$ is consistent with a MDDR scaling $\propto \mu^4$, though several times smaller than the full inelastic MDDR scaling presented in Ref. [22]. $\bar{\beta}$ is consistent with nonmaximally spin-polarized Cr (1.1×10^{-10} cm^3/s) [22] and with 500 mK inelastic Er and Tm collision rates, 3.0 and 1.1 $\times 10^{-10}$ cm^3/s, respectively [17]; the large magnitude of the latter rates are attributed to anisotropic electrostatic-driven spin-relaxation collisions of these lanthanides. Further measurements will aim to elucidate these collisional processes in this complex atomic system [18].

Temperature and density profiles contain unusual features common to both ^{164}Dy and ^{163}Dy MOTs. When care is taken to retroreflect and power balance all pairs of MOT beams, the MOTs are typically 30% fewer in population, though they have a larger mean density (10^{11} versus 10^{10} cm^{-3}) than those with slight misadjustment. In ballistic expansion after extinguishing the MOT, a dual component gas is observed comprised of a dense symmetric core of $\sim$200 μK atoms surrounded by a hot, 2–3 mK shell containing 70% of the atoms. Doppler cooling theory in 1D
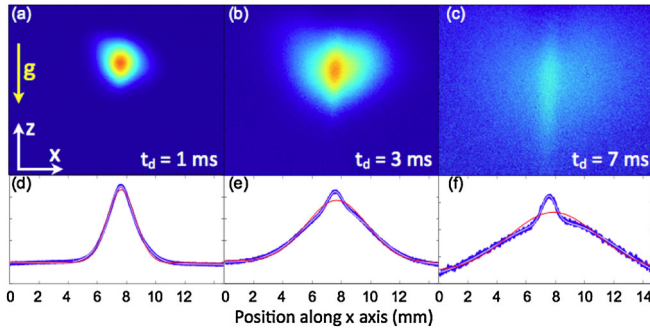
FIG. 4 (color online). (a)–(c) ^{164}Dy absorption images at time t_d after release from MOT revealing a dense stripe with anisotropic temperature. (d)–(f) Column density integrations along $\hat{z}$ versus x. Fits to the data (blue) are to a double (white) and single (red) Gaussian. Additional images in the x-y plane reveal the stripe's azimuthal symmetry.

predicts a cloud temperature of 1.2 mK for the MOT parameters, but comparisons to the Er MOT [21] suggest the entire intra-MOT population should be sub-Doppler cooled to ~100 μK as a consequence of the near equal Landé g factors in the ground and excited states ($\Delta g/g =$ 1.7%). Despite Δg being slightly larger than in Er, numerical 1D sub-Doppler cooling simulations (based on Ref. [21] and references within) indicate sub-Doppler cooling of the entire Dy MOT, accounting for typical size and ∇B. The Er MOT, limited by Zeeman and MOT laser power, contained 500$\times$ fewer atoms; it is possible that the hot shell forms subsequent to the cold inner core, which will be investigated. At $t_m = 2$ s, MT temperatures are 100–300 μK depending on ∇B.

While ultracold cores are observed in other MOTs [23], a unique sub-Doppler cooled structure forms when the Dy MOT beams are slightly misbalanced or misaligned (see Fig. 4). Depending on the particular misadjustment, either a dense vertical or horizontal stripe (or both) appear in the core of the cloud. The outer hot atoms remain at $T^H =$ 2–3 mK temperatures, but the (vertical) stripe population acquires an anisotropic temperature distribution of $T_z^C \approx T^H$ and $T_x^C \lesssim 10$ μK. This latter temperature is consistent the 1D numerical sub-Doppler cooling calculation, but its precise measurement is hampered by the hot cloud presence. We offer no explanation other than to note no detection of stripe spin-polarization in Stern-Gerlach measurements (again hampered by the rapid hot cloud expansion), and that $T_x^C \rightarrow T^H$ as ∇B decreases [18]. Under optimal operating conditions, the Dy MOT phase space density is as large as 10^{-7}.

Future work includes narrow-line cooling to ~1 μK on the 1001-nm line [24] and loading into a crossed optical dipole trap. Once optically confined, the large MT losses might be avoided by trapping in the lowest energy Zeeman state. Collision rates in the single partial wave regime will be measured before attempting to evaporatively cool to degeneracy. Ultracold Dy will open new avenues for research in quantum gases and information, and precision measurement.

[1] I. Bloch, J. Dalibard, and W. Zwerger, Rev. Mod. Phys. **80**, 885 (2008).

[2] E. Fradkin et al., arXiv:0910.4166.

[3] T. Miyakawa, T. Sogo, and H. Pu, Phys. Rev. A **77**, 061603(R) (2008); B. M. Fregoso et al., New J. Phys. **11**, 103003 (2009); J. Quintanilla, S. T. Carr, and J. J. Betouras, Phys. Rev. A **79**, 031601(R) (2009).

[4] S. Ospelkaus et al., Faraday Discuss. **142**, 351 (2009).

[5] B. M. Fregoso and E. Fradkin, Phys. Rev. Lett. **103**, 205301 (2009).

[6] W. C. Martin, R. Zalubas, and L. Hagan, *Atomic Energy Levels—The Rare Earth Elements* (NSRDS-NBS, Washington, DC, 1978), Vol. 60.

[7] Unfortunately, Tb exists as a single bosonic isotope, and is susceptible to incoherent 400 K blackbody radiation.

[8] B. Newman et al. (to be published).

[9] N. A. Leefer et al., in *Proceedings of the 7th Symposium on Frequency Standards and Metrology*, edited by L. Maleki (World Scientific, Singapore, 2009), pp. 34–43.

[10] H. J. Metcalf and P. van der Straten, *Laser Cooling and Trapping* (Springer-Verlag, New York, 1999).

[11] T. Lahaye et al., Nature (London) **448**, 672 (2007).

[12] S. Yi, T. Li, and C. Sun, Phys. Rev. Lett. **98**, 260405 (2007).

[13] L. Sadler et al., Nature (London) **443**, 312 (2006).

[14] G. Baym and T. Hatsuda (private communication).

[15] J. J. McClelland and J. L. Hanssen, Phys. Rev. Lett. **96**, 143005 (2006).

[16] A. Derevianko and C. Cannon, Phys. Rev. A **70**, 062319 (2004); M. Saman and K. Mlmer, ibid. **78**, 012336 (2008).

[17] C. B. Connolly et al., Phys. Rev. A **81**, 010702(R) (2010).

[18] S.-H. Youn, M. Lu, U. Ray, and B. L. Lev (to be published).

[19] Linewidth $\Gamma/2\pi = 31.9 \pm 0.7$ MHz; see Refs. [6,18].

[20] R_1/Γ is consistent with Er's and 4$\times$ smaller than that numerically estimated [V. Flambaum (private communication)].

[21] A. J. Berglund, S. A. Lee, and J. J. McClelland, Phys. Rev. A **76**, 053418 (2007).

[22] S. Hensler et al., Appl. Phys. B **77**, 765 (2003).

[23] K. Kim et al., Phys. Rev. A **69**, 033406 (2004).

[24] A. J. Berglund, J. L. Hanssen, and J. J. McClelland, Phys. Rev. Lett. **100**, 113002 (2008).

[25] N. Leefer, A. Cingoz, and D. Budker, Opt. Lett. **34**, 2548 (2009).